VTT Technical Research Centre of Finland

Optimization of podded propulsor for fast ropax using RANS solver with cavitation model

Sanchez-Caja, Antonio; Pylkkänen, Jaakko

Published in:
Proceedings of the 8th International Conference on Fast Sea Transportation, FAST 2005

Published: 01/01/2005

Document Version
Peer reviewed version

InternationalConference on Fast Sea Transportation
FAST'2005, June 2005, St.Petersburg, Russia

Optimization of Podded Propulsor for Fast Ropax Using RANS Solver with Cavitation Model

Antonio Sánchez-Caja & Jaakko V. Pylkkänen
VTT Industrial Systems
Tietotie 1 C, Espoo P.O. Box 17053, Finland

ABSTRACT

Within EU Project FASTPOD the application of podded propulsors to high speed commercial vessels has been studied. In particular a Ropax and a cargo ship were selected as merchant ship candidates for the near future with speeds in the range of 35-38 knots. For such high speeds the hydrodynamic design of the propeller with its housing is critical due to the appearance of cavitation both on the propeller blades and pod housing. The paper deals with the design process of the propeller and housing for the Ropax vessel using RANS solver FINFLO. A one-phase cavitation model has been implemented, which combines a linearized kinematic boundary condition for the tangentiality of the flow at the bubble surface with a constant pressure boundary condition in the cavitation bubble. The simplicity of the model allows a reasonable prediction of cavitation extent without a significant increase of computational effort. Good performance from a cavitation standpoint both on the strut and propeller blades usually results in reduced propulsor efficiency. For this particular application a compromise is made to get satisfactory performance from both cavitation and efficiency point of view.

INTRODUCTION

In fast ship applications one of the main concerns for a propeller designer is cavitation control. Extensive cavitation not only reduces propulsor efficiency but also results in radiated noise and material corrosion. The risk of cavitation on the propeller blades has been traditionally reduced by decreasing the blade loading. This has been made in different ways: distributing the propulsion load among several propulsion units, increasing the number of propellers per propulsion unit (CRP, tandem propellers), transferring part of the loading to control surfaces (stators, ducts), etc; and for a given propeller, increasing the expanded area ratio, decreasing the design loading (circulation) at the blade tips, etc.

For podded propulsors cavitation can be present not only on the propeller surface but also on the components of the housing. For tractor type podded units sheet, streak or bubble cavitation may appear on the strut suction side due to the combined effect of the relatively large thickness to chord ratio of the strut profile and the accelerated, oblique flow in the propeller slipstream caused by the propeller-induced axial and tangential velocities. If fins are present, the same type of cavitation may appear on their surfaces and also fin tip vortex cavitation may occur. Lack of smoothness on the pod surfaces may lead to streak cavitation on areas of abrupt geometry changes. Moreover hub vortex cavitation attached as a tail to the pod body may also be present due to the transference of the blade root loading (circulation) to the downstream end of the pod.

From the standpoint of cavitation on the propeller blades themselves, tractor pods show unique features also. Steep conical hubs typical of tractor units alter considerably the direction of the inflow to the profile sections at the root of the blade. For this reason the local flow in this region should be accurately modeled if root cavitation is to be avoided. Additionally the hull wake at the propeller plane is usually very small, which results in an increase of the margin for the cavitation-free operation.

Another main concern for the designer of tractor podded propulsors is the need to obtain good figures of efficiency. With the technology available at the beginning of the FASTPOD project large pods with delivered power over 25 MW were considered as starting point for the investigation. Pods of large diameter produce significant drag losses and limit the capability for the propeller to provide thrust due to the increase of the hub-propeller diameter ratio. With the advance of technology their size is expected to be reduced in the near future by use of cryogenic motors.

In this paper the development of the pod/propeller design is described. RANS code FINFLO is used as analysis tool for the assessment of the hydrodynamic quality of the alternatives studied. Special emphasis was set on reducing cavitation while keeping efficiency within acceptable limits. Initial design

iterations for the housing for this particular case were reported in Sánchez-Caja, et al. (2004).

1. NUMERICAL METHOD

1.1. Governing equations

The flow simulation in FINFLO is based on the solution of the RANS equations by the pseudo-compressibility method. FINFLO solves the RANS equations by a finite volume method. The solution is extended to the wall and is based on approximately factorized time-integration with local time-stepping. The code uses either Roe's flux-difference splitting or Van Leer's flux-vector splitting. A multigrid method is used for the acceleration of convergence. Solutions in coarse grid levels are used as starting point for the calculation in order to accelerate convergence. A detailed description of the numerical method including discretization of the governing equations, solution algorithm, etc. can be found in Sanchez-Caja et al. (1999 and 2000). Chien's low Reynolds number k-epsilon model has been used in the calculation.

1.2. Cavitation model

A one-phase cavitation model has been implemented, which combines a linearized kinematic boundary condition for the tangentiality of the flow at the bubble surface with a constant pressure boundary condition in the cavitation bubble. The simplicity of the model allows a reasonable prediction of cavitation extent without a significant increase of computational effort. Inside the vapor bubble the pressure is set equal to the vapor pressure and no frictional forces are active on adjacent solid surfaces.

1.3. Other boundary conditions

Two types of computations were made. For the first stages of the design alternative housing geometries were studied subjected to an inflow defined from the conditions in the propeller slipstream at a distance corresponding to the location of the maximum thickness of the strut. In other words, the propeller was modeled by inlet boundary conditions. For these calculations no interaction effects between the strut and the propeller were considered. In order to implement properly the inlet boundary condition on the inflow a cylinder was placed in front of the propeller plane. The flow was allowed to slip over the cylinder so as to prevent a non-physical growth of the boundary layer. The streamwise gradients of the flow variables as well as the pressure difference are set to zero at the outlet.

For the second set of calculations the entire podded propulsor was modeled and the calculations were based on a steady-state approach in which the flow is circumferentially averaged through a sliding surface located between the propeller and the strut.

2. NUMERICAL SIMULATION

2.1. Computational mesh

Concerning the computational size grids of about 3.4 millions cells were built for alternative housing geometries used in the first set of calculations. However, the design process was speeded up by making the preliminary calculations with coarser grids of about 0.43 million cells corresponding to a coarse level of the original grids, in which every other grid line was removed. The fine grids were used only at the final stage and only for the best hydrodynamic configurations to ascertain the hydrodynamic quality of the final geometry.

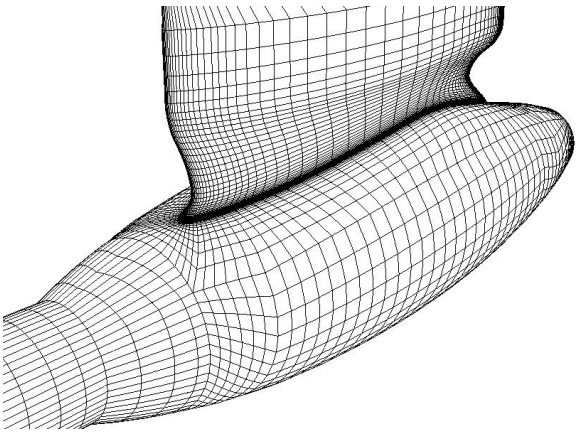

Fig. 1: *Coarse grid used in the design first stages. The strut is asymmetric, (Sánchez-Caja et al., 2004).*

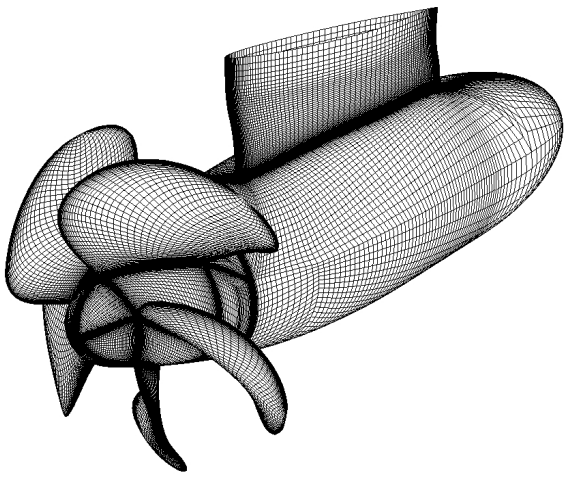

Fig. 2: *Fine grid used in the final stages of the design. The strut is asymmetric.*

For the second group of computations, i.e. entire podded propulsors, the size of the fine mesh was about 7 million cells and the coarse one about 0.9 million cells. The meshes were of O type around the strut and H type around the propeller blades. All the present calculations were made at model scale.

Figures 1 and 2 show the computational meshes on the surfaces of the housing and propeller for the two types of grids used.

2.2. Computation results

The final computations were made in a PC cluster using processors of 3 GHz in Windows environment. As an example, Figure 3 illustrates the convergence history of overall momentum forces in the direction of the propeller axis. It corresponds to computations on a fine grid respectively for the entire podded propulsor.

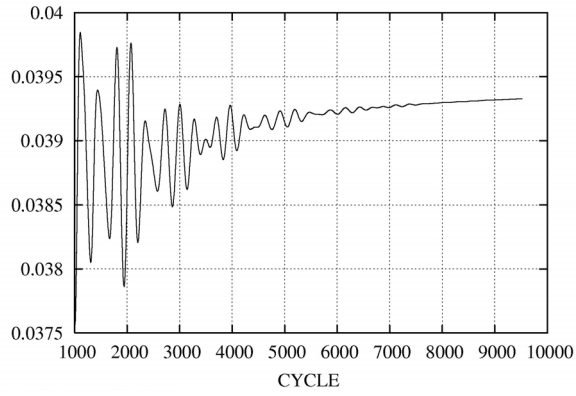

Fig. 3: *Convergence history of overall momentum forces about the propeller axis for the podded propulsor.*

3. GEOMETRY OPTIMIZATION

3.1. Propeller

An initial geometry for the propeller was provided by one of the FASTPOD partners as starting point for the design. It was thought that a 7-bladed propeller could be a good choice for this application. The first RANS calculations showed that it was difficult to obtain a cavitation-free propeller for 38 knots due to the relative high thickness-chord ratio of the sections. Figure 4 shows the extent of cavitation predicted by FINFLO. The areas of cavitation are presented in white color on top of low pressure (black) areas. It was decided to decrease the number of blades to 5 while keeping the same expanded area ratio. The situation improved as shown in Figure 5, which shows some spots of cavitation at the root and near the tip. Then pitch and camber were adjusted to meet the power requirements and to remove the spots of cavitations. The final propeller is shown in Figure 6.

3.2. Pod housing

The first stage of the optimization of the pod housing has been reported in Sánchez-Caja et al. (2004). In summary the strut geometry provided as starting point for the optimization was found to cavitate both on the pressure and suction sides. Then a design philosophy of strut unloading was followed, which resulted in an asymmetric strut with wide cavitation-free margin for the design condition.

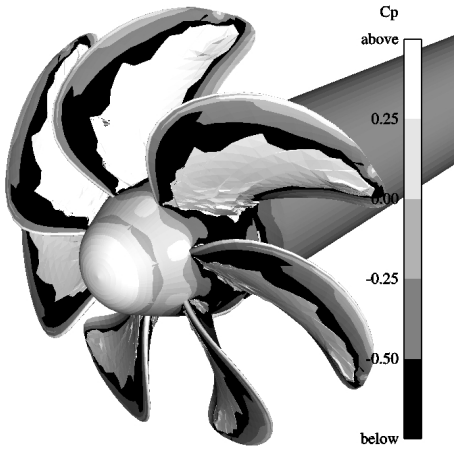

Fig. 4: *Cavitation paterns predicted for the initial 7-bladed propeller.*

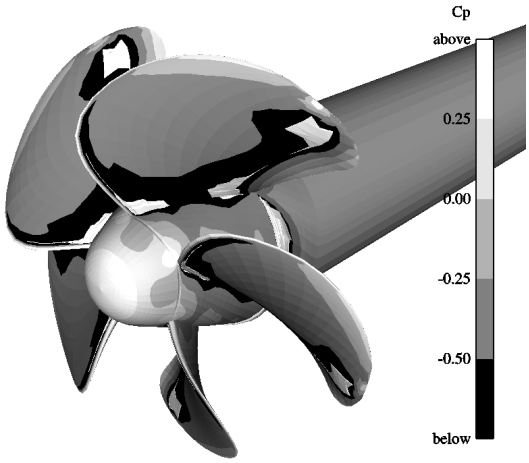

Fig. 5: *Cavitation paterns predicted for the first iteration 5-bladed propeller.*

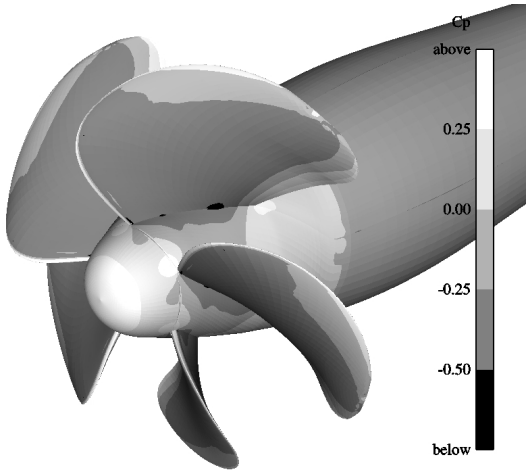

Fig. 6: *Cavitation paterns predicted for the final 5-bladed propeller.*

3.3. Propeller + Pod housing

RANS computations were made at model scale for the complete podded propulsor in a steady-state condition obtained as indicated in section 1.3. The wake resulting from the strut on the propeller plane was very small due also to the unloading of the strut, so the results were not expected to differ much from a time-accurate calculation. The reference pressure for the calculation was adjusted to simulate the full scale conditions at r/R=0.7 when the propeller blade is set to the 12 o'clock position.

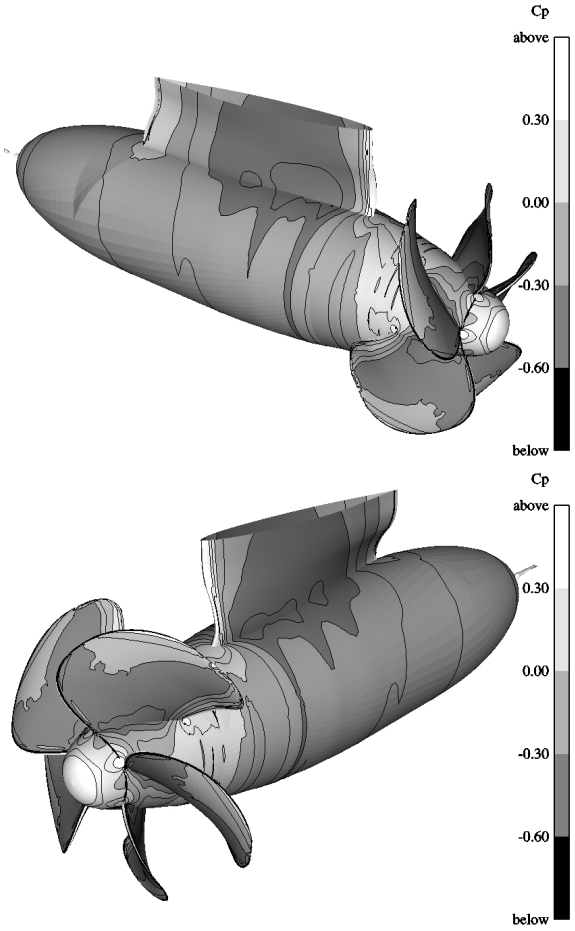

Fig. 7: *Pressure distribution predicted for the tested 5-bladed propeller and housing. A cavitating tail vortex is shown behind the pod.*

The results showed cavitation-free operation on propeller and strut at the design condition. However, hub vortex cavitation was apparent at the downstream edge of the pod. As the reference pressure was not adjusted at the location of the hub vortex, the strength of the cavitation is expected to be smaller than that shown by the computation. Figure 7 shows the pressure distribution and the tail vortex cavitation at the edge of the pod. The calculations showed large drag on the pod housing that make it difficult to meet the design requirements. The large drag was a consequence of the large pod-propeller diameter ratio. In particular, blade tip unloading, i.e. load transfer to the root, combined with strut unloading resulted in large hub-vortex drag.

In order to decrease the pod drag a strut with carefully defined load distribution to avoid cavitation at straight ahead condition was designed. The effect of the new strut was twofold. On the one hand the load on the strut reduces the strut drag. On the other hand it decreases considerably the hub drag by recovering the rotational energy on the propeller slipstream to such an extent that the tail vortex cavitation disappears downstream of the pod. RANS calculation showed no cavitation at the design condition for the steady state calculation. Even though no calculations were made for off-design conditions, it is expected that the cavitation margin is not wide at moderate steering angles for such high speed.

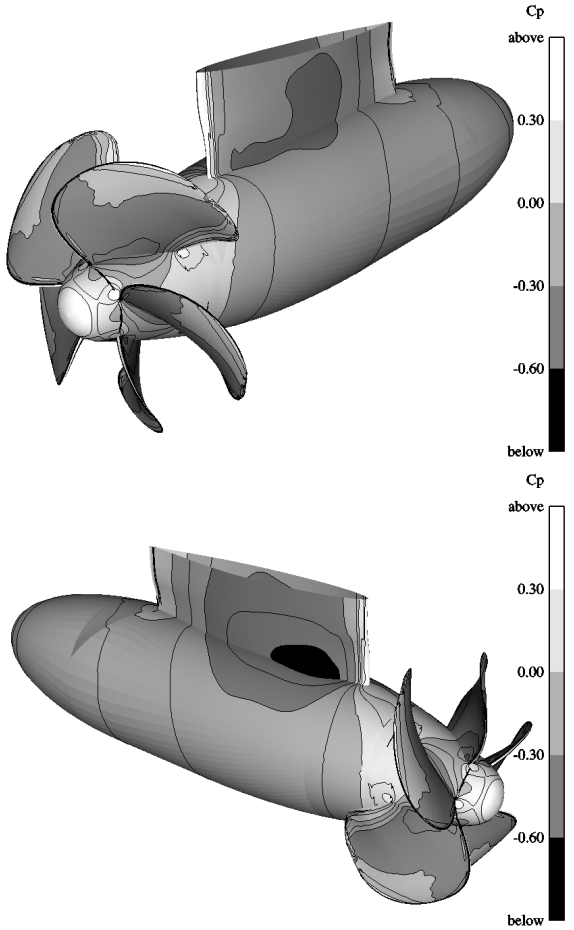

Fig. 8: *Pressure distribution predicted for the final 5-bladed propeller and housing.*

Open water test have been made for the podded propulsor with unloaded strut at HSVA. No turbulence stimulation was employed. Table I shows the differences in percentages between calculations and experiments. As the calculations were made with the cavitation model on, and in the experiments no cavitation was considered a second calculation was

made switching off the cavitation model. The difference between predicted and calculated values was 3.0 percent for the unit thrust, 0.7 for the propeller/unit torque and 2.4 for the efficiency. From the table it can be noticed that the cavitation model reduces the hub drag (i.e. increase the unit thrust) as the pressure is not allowed to decrease below the vapor pressure at the pod rear end.

Table I. Open water calculations for podded propulsor with unloaded strut. Differences from measurements in %.

	Cavitation ”on”	Cavitation ”off”
Kt-unit	-1.5	-3.0
Kq	-0.8	-0.7
η	-0.7	-2.4

Table II. Calculated drag reductions in % for the components of the final housing relative to those of the initial housing and to the total blade thrust.

	Component	Blade
Pod	25	6.7
Strut	12	0.9

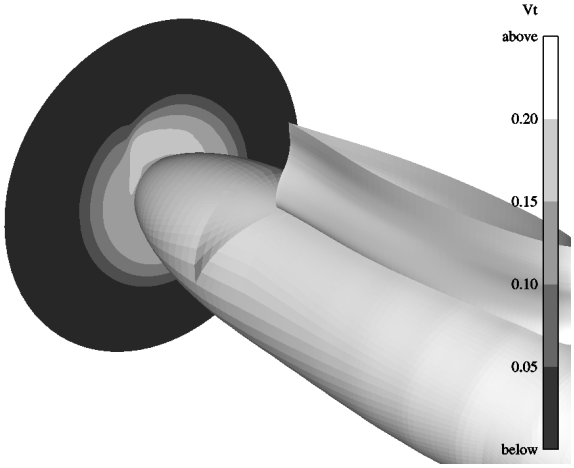

Fig. 9: *Propeller- induced tangential velocity on a plane at the back end of the pod. Geometry of the unloaded strut. Upper view.*

RANS calculations were also made for the final propeller and housing. Table II shows percentages of drag reduction for the final housing. The pod drag is reduced in 25 percent, which is equivalent to a 6.7 percent of the thrust given by the blades. For the strut the corresponding percentages are 12 and 0.9. The thrust and torque of the propeller blades are not affected by the shape of the strut. The strong reduction of pod drag derives from the recovery of rotational energy from the asymmetric strut. The calculations point to a significant increase of the unit efficiency, which permits to meet the design power requirements in straight ahead condition.

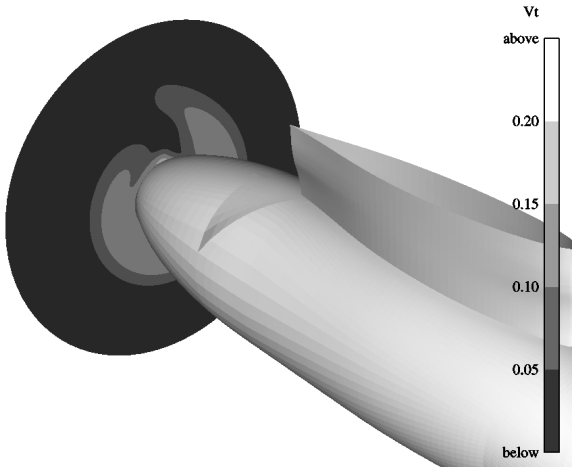

Fig. 10: *Propeller- induced tangential velocity on a plane at the back end of the pod. Final geometry. Upper view.*

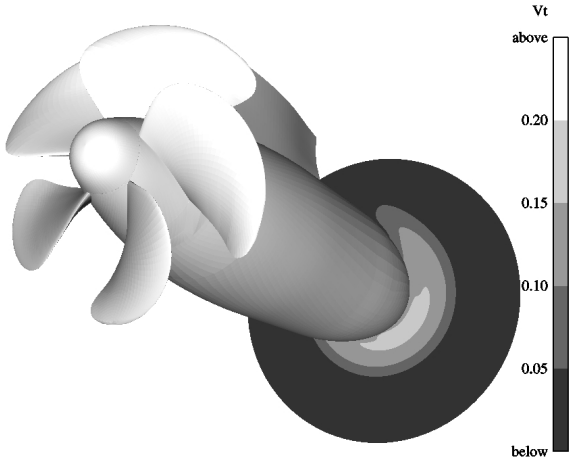

Fig. 11: *Propeller- induced tangential velocity on a plane at the back end of the pod. Final geometry. Lower view.*

Generally the prediction of absolute forces for a RANS code is more difficult than the prediction of relative changes in forces when comparing two propeller versions for a particular application. As the correlation between calculated and measured values was surprisingly good for the unloaded strut, the comparison between calculated values for the two podded propulsion versions is expected to be accurate.

Figures 9, 10 and 11 show the tangential propeller-induced velocities at the rear end of the pod. Strong reduction of tangential velocity is apparent at the angular position aligned with the shadow of the strut for the final geometry as compared to that of the

unloaded strut. Additional fins for the recovery of rotational energy may be fitted at other angular locations, but their design should be made very carefully in order not to increase the total drag of the propulsion unit.

4. DISCUSSION

For the design of a cavitation-free propeller with large hub-propeller diameter ratio for high-speed operation it is desirable to use circulation distributions with unloaded tips. In principle from the standpoint of *blade* efficiency tip unloading not necessarily means strong reduction of efficiency. It depends on how such reduction is made. In fact lifting line calculations show slightly higher *blade* efficiency for *optimum* circulation distributions with non-zero values at the root as compared with those where the circulation vanishes (Kerwin, 1964). However, such distributions are generally not used since they result in lower *propeller* efficiency due to the generation of hub vortex drag or since they may lead to root cavitation in the case of large loadings.

The results presented in this investigation show that for some particular applications in which the blade root circulation can be partially absorbed before becoming hub vortex, moderate root loading may mean a compromise between good efficiency and good cavitation behavior.

CONCLUSIONS

The design of a propeller for speeds about 38 knots with good efficiency and at the same time free of cavitation is a difficult task. Measures directed to improving cavitation performance may be in conflict with those aimed at increasing propulsor efficiency. Large pod-propeller diameter ratios impose a penalty on propeller efficiency. Unloaded struts present good characteristics from the cavitation viewpoint. However, when combined with large pods and blade root loading they may result in low figures of efficiency. Asymmetric struts with carefully design hydrodynamic load may contribute to the recovery of rotational losses in the propeller slipstream and to the significant decrease of pod vortex drag.

ACKNOWLEDGMENTS

This work has been made within the European Union FASTPOD project. FASTPOD means Fast Ship Applications for Pod Drives, Framework FP5, Project no: GRD2-2001-50063, number of partners 17, number of participating countries 7. The authors wish to thank the partners in FASTPOD.

REFERENCES

1. Kerwin, J.E. and Leopold, R. *A Design Theory for Subcavitating Propellers*, presented at the annual meeting of the Society of Naval Architects and Marine Engineers, New York, N.Y., November 12-13, 1964.

2. Sánchez-Caja, A., Rautaheimo, P., Salminen, E., and Siikonen, T. *Computation of the Incompressible Viscous Flow around a Tractor Thruster Using a Sliding Mesh Technique*, 7th International Conference in Numerical Ship Hydrodynamics, Nantes 1999.

3. Sánchez-Caja, A., Rautaheimo, P. and Siikonen, T. *Simulation of Incompressible Viscous Flow Around a Ducted Propeller Using a RANS Equation Solver*, 23rd Symposium on Naval Hydrodynamics, Val de Reuil (France), 2000.

4. Sánchez-Caja, A. and Pylkkänen, J. V. *On the Hydrodynamic Design of Podded Propulsors for Fast Commercial Vessels*. The 1st International Conference on Technological Advances in Podded Propulsion April 14-16, 2004, University of Newcastle (U.K.)